

This is an Accepted Manuscript version of the following article, accepted for publication in **HEAT TRANSFER ENGINEERING**.  
Postprint of: Wajs J., Mikielewicz D., Fornalik-Wajs E., Bajor M., High Performance Tubular Heat Exchanger with Minijet Heat  
Transfer Enhancement, HEAT TRANSFER ENGINEERING, Vol. 40, iss. 9-10 (2019), pp. 772-783,  
DOI: [10.1080/01457632.2018.1442369](https://doi.org/10.1080/01457632.2018.1442369)

It is deposited under the terms of the Creative Commons Attribution-NonCommercial License (<http://creativecommons.org/licenses/by-nc/4.0/>),  
which permits non-commercial re-use, distribution, and reproduction in any medium, provided the original work is properly cited.

# **High Performance Tubular Heat Exchanger with Minijet Heat Transfer Enhancement**

JAN WAJS <sup>1</sup>, DARIUSZ MIKIELEWICZ <sup>1</sup>, ELZBIETA FORNALIK-WAJS <sup>2</sup>, and  
MICHAŁ BAJOR <sup>1</sup>

1: Department of Energy and Industrial Apparatus, Gdansk University of Technology, Gdansk, Poland

2: Department of Fundamental Research in Energy Engineering, AGH University of Science and Technology, Krakow, Poland

---

<sup>1</sup> Address correspondence to Dr. Jan Wajs, Gdansk University of Technology, Faculty of Mechanical Engineering, Department of Energy and Industrial Apparatus, ul. Narutowicza 11/12, 80–233 Gdansk, Poland, Tel. +48 583472830, Fax. +48 583472816, E-mail: Jan.Wajs@pg.edu.pl

**ABSTRACT** In the paper the original cylindrical heat exchanger with minijets (MJHE) was introduced. The systematic experimental analysis of the prototype heat exchanger was described with special attention paid to such parameters as the heat transfer effectiveness, heat transfer rates, overall heat transfer coefficients and pressure drop. The heat transfer coefficients were determined on the basis of Wilson plot method, the most suitable approach for heat transfer coefficient determination in exchangers of complex geometry. The thermal-hydraulic characteristics of the in-house manufactured prototype of MJHE in water-water and gas-water configuration was also presented. The experimental results were compared with the predictions from well-known correlations found in the published research papers dedicated to the free-surface and submerged types of jets.

## ***INTRODUCTION***

Captured and reused waste heat is an emission-free substitute for costly purchased fossil fuels or electricity. It can also lead to reduction in emission of greenhouse gases, as the energy will be more efficiently utilized and in such case emissions of CO<sub>2</sub> (the product of complete combustion) will be smaller. Present ecological regulations are already pointing out on significant reductions of CO<sub>2</sub> emissions, while the expected future ones will be even more strict and may cause severe penalties. One of the possible ways of CO<sub>2</sub> emission reduction is utilization of waste energy. It seems to be the best option for currently operating industrial infrastructure, therefore fast development of energy-efficient technologies, especially on the gas side, is observed nowadays. The main industrial sources of waste energy are the exhaust gases and hot water. The energy in the form of heat from these sources can be recovered and utilized (1) to generate electricity, (2) to heat the buildings or processes through the heat exchangers or heat pumps, (3) to cool buildings or processes by the thermally-driven systems [1]. The technologies of waste heat recovery depend on the heat source temperature.



Generally, all waste heat sources can be divided into (1) low temperature ( $<230^{\circ}\text{C}$ ), (2) medium temperature ( $230\text{-}650^{\circ}\text{C}$ ) and (3) high temperature ( $>650^{\circ}\text{C}$ ) levels [1]. From the application point of view the most convenient to manage are the medium and high temperature sources. Analysis of the statistical reports [2] indicates, however, that the low-temperature gaseous heat sources account for about 50% of all waste heat. The gaseous low temperature waste heat recovery technology still needs to be developed, since the methods and their efficiencies are severely limited by the temperature. Therefore developments in the area of high efficiency heat exchangers are one of the best ways to increase the heat recovery from waste heat of low-temperature sources, especially of gaseous origin. In such case, however, efficient heat transfer intensification techniques must be sought. In literature three general methods of heat transfer intensification can be distinguished [3]:

- active (requiring additional energy),
- passive (no additional energy, but the intensification is attained by surface modifications),
- compound enhancement (parallel application of active and passive methods or various passive ones).

Due to the requirement of additional energy in the case of active methods, they are very often applied in the phase change processes, however their control is rather difficult. Examples of active enhancement methods are: stirring the fluid or vibrating the surface [4]. On the other hand examples of passive methods of heat transfer intensification are: change of surfaces roughness [5], application of swirl flow devices [6] or coiled tubes [7] or similar.

Conventional jet impinging heat transfer enhancement technique is very often used in many engineering applications. It allows achieving very high heat transfer rates from a target surface. This technique is commonly applied in metallurgy, cooling of electronic components, processing of materials, cooling of turbine blades, etc. Due to the variety of

applications the jets can be of free-surface or submerged-confined types, single or arranged in the arrays. The medium creating the jets can be of gaseous or liquid origin. Single jet characteristics was analyzed for example by Goldstein et al. [8] or Lee and Lee [9], but the analysis of jets array is more interesting from the point of view of considered here topic. The impingement heat transfer from jets array was widely analyzed by several researchers, and here only a selection of them is mentioned, namely Obot and Trabold [10], Hollworth and Berry [11] or Rhee et al. [12]. It should be noticed that gas jets studies receive a greater attention in studies. Mentioned here can be works due to Viskanta [13], Gulati et al. [14] or Wang et al. [15]. The liquid impinging jets are very important for many applications, also, hence the studies can be mentioned due to Stevens and Webb [16], Garimella and Nenaydykh [17], Nakabe et al. [18] or Whelan and Robinson [19]. The extensive overview of impinging heat transfer enhancement techniques was presented by Martin [20] or Zuckerman and Lior [21]. Implementation, however, of the minijets impingement into the recuperators can be considered as innovative and the systematic studies on that topic were not presented thus far. Application of minijet impingement ensures significantly higher values of heat transfer coefficients as a consequence of hitting by the streams on the heat transfer partition, separating hot and cold fluids. Fluid film, usually laminar, on the partition is locally disturbed by mentioned fluid jets. It is especially very attractive for the system, in which the heat is transferred between gas and liquid, gas and condensing vapor or gas and boiling liquid. It is widely known that on the gas side the values of heat transfer coefficient are significantly lower, limiting the efficiency of recuperation. That, due to the employment of minijets can be improved. Minijet heat exchangers feature high performance, especially at low flow rates of fluids and low temperature differences between them.

In the paper the original cylindrical heat exchanger with minijets is introduced. Its novel construction is the in-house patented design [22]. The systematic experimental analysis of the



prototype heat exchanger will be described especially from the point of view of such parameters as the heat transfer rates, heat transfer coefficients and pressure drop. The heat exchanger was tested with two fluids (water and gas) with a different configuration (water-water, and gas-water). Results of heat transfer calculations were compared with the predictions by correlations available in literature [23–26]. The preliminary results of investigation in water-water system were also presented in [27].

### ***MINIJET HEAT EXCHANGER (MJHE)***

The schematic view of minijet heat exchanger with the hot and cold fluid perforation openings as well as heat conducting wall is shown in Figure 1. The perforation openings are regarded as spaces between marked broken lines, while the full lines represent solid walls. Detailed geometrical characteristics of the exchanger is described in Table 1. It should be mentioned that the exchanger geometry was designed to fulfill requirements of the prototype of domestic heat and power installation with the organic Rankine cycle [28]. The photograph of assembled prototype and pipe with perforation are shown in Figure 2.

### ***EXPERIMENTAL FACILITY***

All the presented tests were carried out at the stand assembled at Gdansk University of Technology, Department of Energy and Industrial Apparatus, which allowed investigations of convective heat transfer between the streams of hot and cold fluids for two configurations, namely water-water and air-water.

#### ***Water-Water System Test Facility***

Schematic view of the test facility is shown in Figure 3. Cold tap water was split into two streams, i.e. one going directly to heat exchanger, while the second one – to electrical heater,

where it was heated to the conditions needed on the hot side inlet of the heat exchanger. In both streams of water the fine filters were installed to purify efficiently water and to protect all other devices at the facility. The electrical heater was precisely controlled and the settings could be smoothly adjusted due to the presence of the autotransformer. The volumetric flow rates were measured by the rotameters with the accuracy class 1. Temperature of hot and cold water at the inlets and outlets was measured using the T-type thermocouples with accuracy at the level of  $\pm 0.1$  K, whose signals were acquired by the data acquisition system. Such level of thermocouples accuracy was obtained due to an individual sensor calibration procedure done by the system of very high accuracy. During experiments the volumetric flow rate of hot and cold water was varied in the range from 100 to 400 litres per hour (lph). The temperature of hot water at the inlet to heat exchanger was set to three levels, namely 40°C, 60 °C and 90°C, whereas the cold water temperature was kept constant in each measurement series and it was equal to 8°C. The selection of temperature settings was guided in accordance with possible temperatures of the potential waste heat source. The pressure drop was measured by the differential pressure transducer with accuracy of 0.25% of the full range (0-20 kPa).

### ***Gas-Water System Test Facility***

The test facility, presented in Figure 4, enabled the thermal-hydraulic investigations of convection between the air and water, where air was the heating medium, while water was the coolant.

In the laboratory stand the airflow was provided by the radial fan which was controlled by the frequency converter. The air was forced through the section of flow measurement (rotameter), heater and the heat exchanger itself. The air heater consisted of two heaters with a total capacity of 1.8 kW precisely controlled by the autotransformer. Flow rate of water section was adjusted by the throttling valve and its measurement was carried out by a mass



flowmeter. Temperature of air and water at the inlets and outlets was measured by T-type thermocouples, whose signals were recorded by an acquisition system. The temperature of hot air at the inlet to heat exchanger was set to three levels, namely 70°C, 100°C and 130°C, whereas the cold water temperature was kept constant in each measurement series and it was equal to 23°C. The temperature settings were selected in accordance with possibly available gaseous low temperature waste heat source. The air pressure drop was measured by means of the micromanometer (0-250 mm H<sub>2</sub>O).

### ***FLOW CHARACTERISTICS***

Generally, the total pressure drop consists of four factors namely the frictional term, elevation term, pressure losses at the test section inlet and outlet ports, and the acceleration term. The last term would be included in the analysis only if the phase change of particular fluid could be observed. Therefore in the case of reported study, the acceleration term was omitted because there was no phase change occurring in the experiments. The gravitational component was not taken into account due to the horizontal position of heat exchangers.

#### ***Hydraulic Characteristics of Water - Water System***

The analysis of flow resistance in water-water configuration was done at constant temperature of heat exchanger on both sides equal to 10°C. The heat exchanger was placed in horizontal position to make the gravitational part of pressure loss negligible. The results are presented in Figure 5. It can be observed that the pressure loss on the cold side was about two times higher than on the hot side. This difference came from the heat exchanger geometry. The hot water was flowing along the heat exchanger only, while the cold one at inlet and outlet was flowing perpendicularly to the heat exchanger axis. These parts caused the most significant pressure drop.

### ***Hydraulic Characteristics of Gas - Water System***

The flow characteristics of hot passage in gas - water configuration is presented in Figure 6. The analysis was conducted for two values of air temperature at the inlet to the heat exchanger, i.e. 70°C and 130°C. The flow characteristics show that for very low flow rates the overall pressure drop was similar at both temperature values. However at higher values of flow rates the resistance increased with increasing temperature. The flow characteristics of cold passage (water side) is the same as in water - water configuration (see Figure 5).

### ***HEAT TRANSFER ANALYSIS***

As it was mentioned above, the analysis of counter-current minijet heat exchanger was conducted for two configurations: water-water, and gas-water. The inlet conditions of both kinds of system were described and discussed in previous section.

### ***Data Reduction***

In the heat exchangers, to calculate average heat transfer coefficients on both sides of heat transfer surface, the temperature measurements at least in few points are required. The temperature sensors should be placed inside device and be attached to the heat exchanging surface. Such sensors location in heat exchangers of complex geometry is very difficult, especially from the tightness point of view. The overall heat transfer coefficient was calculated in the basis of Wilson plot method [29, 30]. This method enables calculation of average heat transfer coefficient in the basis of inlets and outlets temperature measurements and determination of the overall thermal resistance in the heat exchanger. Such approach followed by simple calculation led to the determination of heat transfer coefficients.

The rate of heat in the heat exchanger can be presented in the form:





$$\dot{Q} = U_0 \cdot LMTD \cdot A = \dot{m}_{hot} \Delta h_{hot} = \dot{m}_{cold} \Delta h_{cold} \quad (1)$$

where LMTD denotes Logarithmic Mean Temperature Difference,  $A$  – heat transfer surface.

The overall heat transfer coefficient can be described as:

$$U_0 = \left( \frac{1}{\alpha_{hot}} + \frac{\delta}{\lambda} + \frac{1}{\alpha_{cold}} \right)^{-1} \quad (2)$$

where  $\alpha_{hot}$  and  $\alpha_{cold}$  are heat transfer coefficients for respective mass flow rates,  $\delta$  is the thickness of wall separating two fluids, whereas  $\lambda$  its thermal conductivity.

The log-mean temperature difference can be determined from a relation for the counter-current heat exchanger as:

$$LMTD = \frac{(T_{hot\_in} - T_{cold\_out}) - (T_{hot\_out} - T_{cold\_in})}{\ln \left( \frac{T_{hot\_in} - T_{cold\_out}}{T_{hot\_out} - T_{cold\_in}} \right)} \quad (3)$$

Assuming that the heat transfer is primarily governed by the flow velocities of both fluids, the simple relations for determination of heat transfer coefficient as a function of fluid velocity can be written.

For constant value of  $\dot{m}_{cold}$  and variable value of  $\dot{m}_{hot}$  there is:

$$\alpha_{cold} = const, \alpha_{hot} = C_{hot} w_{hot}^m \quad (4)$$

For constant value of  $\dot{m}_{hot}$  and variable value of  $\dot{m}_{cold}$  there is:

$$\alpha_{hot} = const, \alpha_{cold} = C_{cold} w_{cold}^m \quad (5)$$

where  $w_{hot}$  and  $w_{cold}$  are the respective flow velocities of hot and cold fluids,  $m$  is the exponent depending on the flow character, for example in the case of turbulent flow inside tubes  $m=0.8$ .

For the heating medium the following relation can be formulated:

$$\frac{1}{U_0} = \left( \frac{1}{\alpha_{cold}} + \frac{\delta}{\lambda} \right) + C_{hot} w_{hot}^{-m} \quad (6)$$

or:

$$\frac{1}{U_0} = C_3 + C_{hot} w_{hot}^{-m} \quad (7)$$

where:

$$C_3 = \frac{1}{\alpha_{cold}} + \frac{\delta}{\lambda} \quad (8)$$

for a series where  $\dot{m}_{cold} = \text{const}$ . Assuming new variables, i.e.  $x = w_{hot}^{-m}$  and  $y = 1/U_0$  a linear relation is obtained:

$$y = C_3 + C_{hot} x \quad (9)$$

For cooling side analogical relations can be derived.

The constants  $C_3$  and  $C_{hot}$  can be determined from the equation representing line, when the cooling fluid had a constant volume flow rate with a variable one for heating fluid. Knowing all parameters, the heat transfer coefficient could be determined.

### ***Thermal Characteristics of Water - Water System***

Thermal characteristics (heat transfer coefficients of hot and cold sides versus the mass flux at the inlet to the heat exchanger) of minijet heat exchanger for three analyzed temperatures of hot water are shown in Figures 7 and 8. On both sides the heat transfer coefficient values increase significantly with increasing mass flux up to 3500 W/(m<sup>2</sup>K) on the hot side and up to about 4000 W/(m<sup>2</sup>K) on the cold one. On the hot side, at all temperature difference values the heat transfer coefficient was very similar. On the cold side the highest values of heat transfer coefficient were obtained at the highest temperature difference (90/8°C).

The comparison of heat transfer coefficient values reached at temperature difference (90/8°C) on the partition sides of hot and cold passages is shown in Figure 9. Their values are plotted versus the mass flux. Significant differences between the distributions can be noticed. That is due to the fact that the temperature difference between the wall and impinging jet was significantly smaller in case of the cold fluid than in the case of the hot one. At the same rate of heat and comparable heat transfer surface that leads to higher values of heat transfer coefficient on the cold side.

### ***Thermal Characteristics of Gas - Water System***

The thermal characteristics (heat transfer coefficient of hot and cold passage versus the mass flux at the inlet to heat exchanger) of minijet heat exchanger for three analyzed temperatures of hot air are shown in Figures 10 and 11. On both sides, an increase of the heat transfer coefficient with increasing mass flux could be observed. On the hot side the increasing trend seems to be linear and the difference between values of heat transfer coefficient determined at considered temperature differences in the most extreme case is about 10% and the same at all mass flux values. On the cold side this tendency is opposite – the difference between values of heat transfer coefficient are differing by about 15% at smaller mass flux values whereas the corresponding difference at higher mass flux values is about 10%.

The comparison between heat transfer coefficient values reached at temperature difference (130/23°C) on the partition sides for hot and cold legs is shown in Figure 12. Their values are plotted versus the mass flux. It should be emphasized that in gas-water system the values of heat transfer coefficient are much lower than in the case of water-water system. The high values of heat transfer coefficients on the cold side were obtained at low values of mass flux in comparison with hot side. It was expected since on the hot side the medium is gas. The

reasoning for the discrepancies between the characteristics is the same as in case of water-water system.

### ***UNCERTAINTY ANALYSIS***

The uncertainty analysis of presented experimental investigations was done in systematic manner. Taking into account low number of measurements repetition, but also high repeatability of data, the statistic uncertainties were not considered. The analysis presented in this paper, concentrated on the systematic error analysis. The analysis was based on the principle of uncertainties propagation described by the formula [31,32]:

$$\Delta y = \sqrt{\left(\frac{\partial f}{\partial x_1} \Delta x_1\right)^2 + \left(\frac{\partial f}{\partial x_2} \Delta x_2\right)^2 + \left(\frac{\partial f}{\partial x_3} \Delta x_3\right)^2 + \dots} \quad (10)$$

where  $\Delta x$  is the maximal uncertainty of measuring instrument. The uncertainty of analyzed functions depended on the particular variables uncertainties. In presented case the uncertainties were connected with direct measurements, indirect calculations and withdrawal from the tables (thermo-physical properties). The applied uncertainties of various devices used in experiment were described in the section discussing the experimental facility and procedure.

The results of uncertainties are summarized in Table 2. The relative uncertainty was calculated on the basis of the following equation:

$$\delta y = \frac{\Delta y}{y} \cdot 100\% \quad (11)$$

### ***EVALUATION OF NUSSELT NUMBER PREDICTING CORRELATIONS***

The values of Nusselt number based on the experimental results were compared with predictions of several correlations from the published research papers. These correlations

were constructed for free-surface and submerged types of jet and were proposed in the basis of similarity theory. The equations can be directly used to calculate the mean Nusselt number value. Correlations due to Fabbri and Dhir [23], Liu et al. [24], Robinson and Schnitzler [25] and Meola [26] have been selected for comparison.

Fabbri and Dhir [23] investigated free-surface jet impingement heat transfer, using water and FC-40 as the coolants of circular copper heat surface. They tested ten arrays of jets, which were drilled and were arranged in a circular pattern with a radial and circumferential pitch of 1 mm, 2 mm, and 3 mm. The number of jets corresponded to pitch spacing and was equal to 397, 127, and 61, respectively. The jet diameters varied from 69 to 250  $\mu\text{m}$ . In the basis of experimental results they proposed a correlation using only three independent dimensionless parameters: jet Reynolds and Prandtl numbers together with the geometrical parameter representing the jet pitch and jet diameter ratio.

Liu et al. [24] focused on heat transfer at the stagnation point considering in their analysis the effect of surface tension. Authors conducted the numerical investigations for laminar jets for the Weber number from the range  $2100 < \text{We}_d < 34000$ .

Robinson and Schnitzler [25] studied experimentally the flat surface cooling by the impingement of water circular jet arrays in the free-surface and submerged conditions. Jet diameters of 1 mm were used, with a jet-to-jet spacing 3, 5 and 7 mm. Heater surface averaged heat transfer was recorded for a dimensionless jet-to-target distance in the range  $2 < H/d < 30$  and a Reynolds number of water in range  $650 < \text{Re}_d < 6500$ .

Meola [26] proposed a new, simpler functional relationship between the Nusselt number and the governing parameters of round impinging jets array. Correlation by Meola was found to predict the area-averaged Nusselt number values quite well for gases [33].

Table 3 provides a summary of selected correlations recommended for submerged and confined types of jets, whereas in Figures 13-15 the results of calculations are presented.

The experimental Nusselt number was calculated in the basis of the nozzle exit diameter using the formula

$$\text{Nu}_{\text{exp}} = \frac{\alpha d}{\lambda} \quad (12)$$

Two statistical parameters namely: mean absolute deviation (*MAE*), also called the average positive error, and the mean bias error (*MBE*) were evaluated. *MAE* was defined as the average of the absolute value of each deviation and considered variance of the experimental results from the predictions of models whereas non-dimensional *MBE* considers variance of the experimental results from the predictions of models. Table 4 gives summary of this assessment, considering mentioned above correlations.

Mean absolute error (*MAE*)

$$\text{MAE} = \frac{1}{n} \sum_{i=1}^n |x_{\text{predicted}_i} - x_{\text{experimental}_i}| [-] \quad (13)$$

Mean bias error (*MBE*)

$$\text{MBE} = \frac{1}{n} \sum_{i=1}^n \frac{x_{\text{predicted}_i} - x_{\text{experimental}_i}}{x_{\text{experimental}_i}} \cdot 100 [\%] \quad (14)$$

Regarding water-water configuration significant differences between the experimental values and those predicted from correlations can be observed except the case of hot side and correlation by Fabbri and Dhir [23], for which good correspondence was found. Expression “good correspondence” comes from the fact that 75% of all results were predicted within  $\pm 25\%$ . It should be emphasized that we are aware that this correlation was constructed for free-surface jets, but surprisingly good agreement between results is giving next point to be considered in the future. Whereas, the same correlation in the case of cold side considerably underestimated the Nusselt number value. The reason for such discrepancies in predicted by nearly all mentioned correlations, most probably, originates from the different number of analyzed jets in the array. For example Robinson and Schnitzler in [25] considered an array

of 121 jets, Fabbri and Dhir in [23] number of jet up to about 400, while in presented experimental investigations the heat exchanger contained perforation with 800 openings on the hot and cold sides. Moreover, all described correlations were developed for the case of cooling of hot surfaces, while in the present experimental studies the impinging jets were both cooling and heating the partition wall. Therefore, to understand the heat transfer processes occurring in the considered heat exchanger further analyses will be required.

Considering the gas-water configuration of heat exchanger a very good consistency between the experimental data and prediction by Meola correlation [26] was found. The difference between experimental and predicted values of heat transfer coefficient did not exceed  $\pm 7\%$ .

## ***CONCLUSIONS***

In the paper innovative construction of compact heat exchanger with minijets has been presented. The idea of such heat exchanger was shown with the flow and thermal characteristics of the prototype. The heat exchanger was tested with two fluids, i.e. water and air, in two configurations. Experimental data was also collected and the heat transfer coefficient was calculated using the Wilson plot method. The presented results are very promising, however discrepancy between them and predicted from correlation ones should be verified. It can be done through the extended experimental studies and the numerical analyses. The numerical analysis of such complex geometry can cause a lot of problems, but will be very useful in understanding the flow behavior and its influence on the heat transfer processes, what can support the experimental data in construction of new correlation.

In parallel the heat exchanger design will be submitted for an optimization process with respect to the length of nozzles to reduce the pressure drop and to increase the heat transfer rates. The optimized construction of heat exchanger would be the most suitable for the heat recovery from waste energy sources as an evaporator or a condenser. The next steps will also



result in determination of a general heat transfer correlation for heat exchanger with minijets technology.

### ***NOMENCLATURE***

$A$	-	heat transfer area, $m^2$
$A_n$	-	total nozzle area, $m^2$
$C$	-	constant in Wilson's methodology
$C_f$	-	flow coefficient
$C_p$	-	specific heat at constant pressure, $J/(kg \cdot K)$
$d$	-	nozzle diameter, m
$f$	-	relative nozzle area, $= (n \cdot 0.25 \cdot \pi \cdot d^2) / A$
$G$	-	mass flux, $kg/(m^2 \cdot s)$
$H$	-	distance between nozzle and impingement surface, m
$h$	-	specific enthalpy, $J/kg$
$LMTD$	-	Logarithmic Mean Temperature Difference, K
$MAE$	-	mean absolute error
$MBE$	-	mean bias error, %
$MJHE$	-	minijets heat exchanger
$m$	-	exponent in Eqs. (4-7)
$\dot{m}$	-	mass flow, $kg/s$
$n$	-	number of nozzles
$Nu$	-	Nusselt number, $= (\alpha d) / \lambda$
$P$	-	pressure, kPa
$Pr$	-	Prandtl number, $= (\mu \cdot C_p) / \lambda$



$\dot{Q}$	-	rate of heat, W
Re	-	Reynolds number, $= (\dot{m} \cdot d) / (A_n \cdot \mu)$
$S$	-	nozzle-to-nozzle spacing, m
$T$	-	temperature, °C
$t$	-	thickness of heat conducting wall, m
$U_0$	-	overall heat transfer coefficient, $W/(m^2 \cdot K)$
$\dot{V}$	-	volumetric flow rates, l/h, $m^3/h$
$v$	-	velocity in nozzle, m/s
$w$	-	velocity at the inlet of MJHE, m/s
We	-	Weber number, $= (\rho \cdot v^2 d) / \sigma$

#### ***Greek letters***

$\alpha$	-	heat transfer coefficient, $W/(m^2 \cdot K)$
$\Delta$	-	difference value
$\delta$	-	wall thickness, m
$\lambda$	-	thermal conductivity of fluid, $W/(mK)$
$\mu$	-	dynamic viscosity of fluid, Pa·s
$\rho$	-	density, $kg/m^3$
$\sigma$	-	surface tension, N/m

#### ***Subscripts***

<i>cold</i>	-	in regard to cold fluid
<i>d</i>	-	based on nozzle diameter
<i>exp</i>	-	experiment
<i>hot</i>	-	in regard to hot fluid
<i>in</i>	-	inlet



$L$  - length in Robinson and Schnitzler correlation  
 $out$  - outlet

## **REFERENCES**

- [1] Zhou, N., Wang, X., Chen, Z., and Wang Z., Experimental Study on Organic Rankine Cycle for Waste Heat Recovery from Low-Temperature Flue Gas, *Energy*, vol. 55, pp. 216-225, 2013.
- [2] BCS Inc., Waste Heat Recovery: Technologies and Opportunities in U.S. Industry, US Dept. of Energy (DOE), 2008.
- [3] Bergles, A.E., ExHFT for fourth generation heat transfer technology, *Experimental Thermal and Fluid Science*, vol. 26, pp. 335-344, 2002.
- [4] Nesis, E.I., Shatalov, A.F., and Karmatskii, N.P., Dependence of the Heat Transfer Coefficient on the Vibration Amplitude and Frequency of a Vertical Thin Heater, *Journal of Engineering Physics and Thermophysics*, vol. 67, pp. 696-698, 1994.
- [5] Wajs, J., and Mikielwicz, D. Influence of Metallic Porous Microlayer on Pressure Drop and Heat Transfer of Stainless Steel Plate Heat Exchanger, *Applied Thermal Engineering*, vol. 93, pp. 1337-1346, 2016.
- [6] Tiruselvam, R., and Vijay R.R., The Tube Side Heat Transfer Coefficient for Enhanced Double Tube by Wilson Plot Analysis, *Journal of Applied Sciences*, vol. 11, pp. 1725-1732, 2011.
- [7] Purandare, P.S., Lele, M.M., and Gupta R.K., Investigation on Thermal Analysis of Conical Coil Heat Exchanger, *Int. Journal Heat Mass Transfer*, vol. 90, pp. 1188-1196, 2015.
- [8] Goldstein, R.J., Sobolik, K.A., and Seol, W. S., Effect of Entrainment on the Heat Transfer to a Heated Circular Air Jet Impinging on a Flat Surface, *Journal of Heat Transfer*, vol. 112, pp. 608-611, 1990.

- [9] Lee, J., and Lee S.J., Stagnation Region Heat Transfer of a Turbulent Axisymmetric Jet Impingement, *Experimental Heat Transfer*, vol. 12, pp. 137-156, 1999.
- [10] Obot, N.T., and Trabold, T.A., Impingement Heat Transfer within Arrays of Circular Jets, Part 1: Effects of Minimum, Intermediate, and Complete Crossflow for Small and Large Spacings, *Journal of Heat Transfer*, vol. 109, pp. 872-879, 1987.
- [11] Hollworth, B. R., and Berry, R. D., Heat Transfer from Arrays of Impinging Jets with Large Jet-to-Jet Spacing, *Journal of Heat Transfer*, vol. 100, pp. 352-357, 1978.
- [12] Rhee, D.H., Yoon, P.Y., and Cho, H. C., Local Heat/Mass Transfer and Flow Characteristics of Array Impinging Jets with Effusion Holes Ejecting Spent Air, *Int. Journal Heat Mass Transfer*, vol. 46, pp. 1046-1061, 2003.
- [13] Viskanta, R., Heat Transfer to Impinging Isothermal Gas and Flames Jets, *Experimental Thermal and Fluid Science*, vol. 6, pp. 111-134, 1993.
- [14] Gulati, P., Katti, V., and Prabhu, S.V., Influence of the Shape of the Nozzle on Local Heat Transfer Distribution Between Smooth Flat Surface and Impinging Air Jet, *Int. Journal of Thermal Sciences*, vol. 48, pp. 602-617, 2009.
- [15] Wang, X.L., Motala, D., Lu, T.J., Song, S.J., and Kim, T., Heat Transfer of a Circular Impingement Jet on a Circular Cylinder in Crossflow, *Int. Journal of Thermal Sciences*, vol. 78, pp. 1-8, 2014.
- [16] Stevens, J., and Webb, B.W., Measurements of the Free Surface Flow Structure Under an Impinging, Free Liquid Jet, *Journal of Heat Transfer*, vol. 114, pp. 79-84, 1992.
- [17] Garimella, S.V., and Nenaydykh, B., Nozzle-Geometry Effects in Liquid Jet Impingement Heat Transfer, *Int. Journal Heat Mass Transfer*, vol. 39, pp. 2915-2923, 1996.
- [18] Nakabe, K., Fornalik, E., Yamamoto, Y., Ohta, T., Eschenbacher, J.F., and Suzuki, K., Interactions of Longitudinal Vortices Generated by Twin Inclined Jets and Enhancement of Impingement Heat Transfer, *Int. Journal of Heat and Fluid Flow*, vol. 22, pp. 287-292, 2001.



- [19] Whelan, B.P., and Robinson, A.J., Nozzle geometry effects in liquid jet array impingement, *Applied Thermal Engineering*, vol. 29, pp. 2211-2221, 2009.
- [20] Martin, H., Heat and Mass Transfer Between Impinging Gas Jets and Solid Surfaces, in *Advances in Heat Transfer*, vol. 13, pp. 1-60, 1977.
- [21] Zuckerman, N., and Lior, N., Jet Impingement Heat Transfer: Physics, Correlations, and Numerical Modeling, *Advances in Heat Transfer*, vol. 39, pp. 565-631, 2006.
- [22] Wajs, J., Mikielwicz, D., and Fornalik-Wajs, E., Microjet Heat Exchanger with a Cylindrical Geometry, Especially for Heat Recovery from Low-Temperature Waste Energy Sources, Polish patent, PL224494, 2013 (in Polish).
- [23] Fabbri, M., and Dhir, V.K., Optimized Heat Transfer for High Power Electronic Cooling Using Arrays of Microjets, *Journal of Heat Transfer*, vol. 127, pp. 760-769, 2005.
- [24] Liu, X., Gabour, L.A., and Lienhard J.H., Stagnation Point Heat Transfer During Impingement of Laminar Liquid Jets: Analysis Including Surface Tension, *Journal of Heat Transfer*, vol. 115, pp. 99-105, 1993.
- [25] Robinson, A.J., and Schnitzler, E., An Experimental Investigation of Free and Submerged Miniature Liquid Jet Array Impingement Heat Transfer, *Experimental Thermal and Fluid Science*, vol. 32, pp 1-13, 2007.
- [26] Meola, C., A New Correlation of Nusselt Number for Impinging Jets, *Heat Transfer Engineering*, vol. 30, pp. 221-228, 2009.
- [27] Wajs, J., Mikielwicz, D., Fornalik-Wajs, E., and Bajor, M., Recuperator with Microjet Technology as a Proposal for Heat Recovery from Low-Temperature Sources. *Archives of Thermodynamics*, vol. 36, no. 4, pp. 49-64, 2015.
- [28] Wajs, J., Mikielwicz, D., Bajor, M., and Kneba, Z., Experimental Investigation of Domestic Micro-CHP Based on the Gas Boiler Fitted with ORC Module, *Archives of Thermodynamics*, vol. 37, no. 3, pp. 79-93, 2016.



- [29] Wilson, E.E., A Basis for Rational Design of Heat Transfer Apparatus. *Trans. ASME J. Heat Transfer*, vol. 37, pp. 47-82, 1915.
- [30] Fernandez-Seara, J., Uhia, F.J., Sieres, J., and Campo, A., A general Review of the Wilson Plot Method and its Modifications to Determine Convection Coefficients in Heat Exchange Devices, *Applied Thermal Engineering*, vol. 27, pp. 2745-2757, 2007.
- [31] Tatara, R., and Lupia, G., Assessing Heat Exchanger Performance Data Using Temperature Measurement Uncertainty, *International Journal of Engineering, Science and Technology* vol. 3, pp. 1-12, 2011.
- [32] Zieba, A., *Analysis of the Data in Science and Technology*, PWN, Warszawa, 2013 (in Polish).
- [33] Michna, G.J., Browne, E.A., Peles, Y., and Jensen, M.K., The Effect of Area Ratio on Microjet Array Heat Transfer. *Int. Journal of Heat and Mass Transfer*, vol. 54, pp. 1782-1790, 2011.

**Table 1** Geometrical characteristics of MJHE heat transfer area

Dimension	Size
length of heat conducting wall (m)	0.281
outer diameter of heat conducting wall (m)	0.018
thickness of heat conducting wall, $t$ (m)	0.001
nozzle diameter, $d$ (m)	0.001
heat transfer area, $A$ (m <sup>2</sup> )	0.015
number of nozzles (hot/cold passage), $n$	752 / 820
distance between nozzle and impingement surface (hot/cold passage), $H$ (m)	0.002 / 0.001
nozzle-to-nozzle spacing, $S$ (m)	0.004

**Table 2** Values of maximal error for both analysed configurations

Parameter	Relative value [%]
<b>Water-Water System</b>	
volumetric flow rates	4.20
pressure drop	3.81
rate of heat	8.19
heat transfer coefficients (hot passage)	5.59
heat transfer coefficients (cold passage)	8.04
Reynolds number (hot passage)	5.22
Reynolds number (cold passage)	5.21
<b>Gas-Water System</b>	
volumetric flow rates of air	7.78
mass flow rate of water	1.16
pressure drop	1.10
rate of heat	10.14
heat transfer coefficients (hot passage)	4.05
heat transfer coefficients (cold passage)	6.91
Reynolds number (hot passage)	7.80
Reynolds number (cold passage)	2.21

**Table 3** Selected correlations for Nusselt number

Author(s)	Nusselt correlation	Remarks
Fabbri and Dhir [23]	$\text{Nu} = 0.043 \cdot \text{Re}_d^{0.78} \cdot \text{Pr}^{0.48} \exp\left(-0.069 \frac{S}{d}\right)$	fluids: water, FC40 $43 \leq \text{Re}_d \leq 3813$ ; $2.6 \leq \text{Pr} \leq 84$ ; $4 \leq \frac{S}{d} \leq 26.2$
Liu et al. [24]	$\text{Nu} = 0.745 \text{Re}_d^{1/2} \text{Pr}^{1/3}$	laminar jets $2100 < \text{We}_d < 34000$
Robinson and Schnitzler [25]	$\text{Nu}_L = 23.39 \text{Pr}^{0.4} \text{Re}_d^{0.46} \left(\frac{S}{d}\right)^{-0.442} \left(\frac{H}{d}\right)^{-0.00716}$ $\text{Nu} = 0.0635 \text{Nu}_L$	fluids: water submerged jets $2 \leq \frac{H}{d} \leq 3$ ; $3 \leq \frac{S}{d} \leq 7$ ; $650 \leq \text{Re}_d \leq 6500$
Meola [26]	$\text{Nu} = 0.3 \text{Pr}^{0.42} \text{Re}_d^{0.68} C_f^{0.56} \left(\frac{H}{d}\right)^{-0.3} f^{0.15}$	$1.6 \leq \frac{H}{d} \leq 20$ ; $0.0008 \leq f \leq 0.2$ ; $200 \leq \text{Re}_d \leq 10000$



**Table 4** Summary of comparison with correlations from literature

Predicting model	MAE [-]	MBE [%]	% of data within $\pm 25\%$
water/water system - hot passage			
Fabbri and Dhir [23]	0.7	13	75
Liu et al. [24]	13.1	381	0
Robinson and Schnitzler [25]	6.0	175	0
water/water system - cold passage			
Fabbri and Dhir [23]	3.0	-50	0
Liu et al. [24]	8.4	135	0
Robinson and Schnitzler [25]	0.4	-4	0
gas/water system - hot passage			
Meola [26]	0.2	7	100

## List of Figures

**Figure 1** Schematic view of MJHE: 1,3 – perforation opening of hot and cold fluid, respectively, 2 – heat conducting wall, 4 – shell, 5,6 – inlet and outlet of heating medium, 7,8 – inlet and outlet of heated medium.

**Figure 2** View of MJHE and its perforating pipe of hot fluid (A) and cold fluid (B).

**Figure 3** Schematic view of the test stand in water-water configuration.

**Figure 4** Schematic view of the test stand in gas-water configuration.

**Figure 5** Flow characteristics of MJHE in water–water configuration.

**Figure 6** Gas side flow characteristics in gas-water configuration.

**Figure 7** Heat transfer coefficients versus the mass flux for hot passage at the case of water–water configuration.

**Figure 8** Heat transfer coefficients versus the mass flux for cold passage at the case of water–water configuration.

**Figure 9** Comparison of heat transfer coefficients as the mass flux function for the case of water–water configuration at selected temperature difference.

**Figure 10** Heat transfer coefficients versus the mass flux for hot passage at the case of gas–water configuration.

**Figure 11** Heat transfer coefficients versus the mass flux for cold passage at the case of gas–water configuration.

**Figure 12** Comparison of heat transfer coefficients as the mass flux function for the case of gas–water configuration at selected temperature difference.

**Figure 13** Nusselt number versus Reynolds number for water –water configuration, hot (a) and cold (b) passages.

**Figure 14** Comparison of Nusselt number predictions with the presented in this paper experimental data for water –water configuration, hot (a) and cold (b) passages.

**Figure 15** Comparison of the Nusselt number prediction by Meola [26] with the experimental data for gas –water configuration, hot passage.

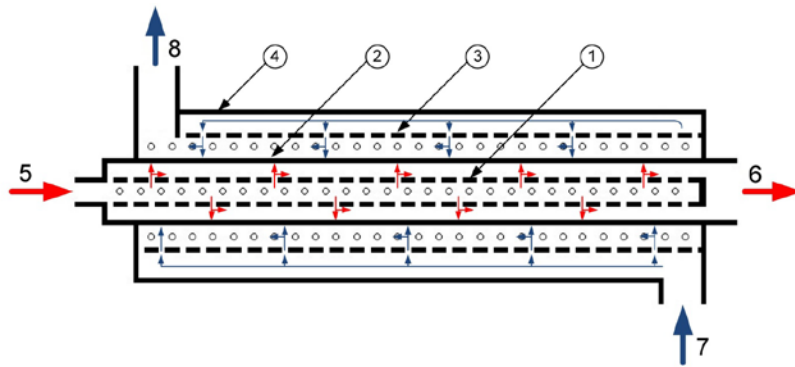


**Figure 1** Schematic view of MJHE: 1,3 – perforation opening of hot and cold fluid, respectively, 2 – heat conducting wall, 4 – shell, 5,6 – inlet and outlet of heating medium, 7,8 – inlet and outlet of heated medium.



**Figure 2** View of MJHE and its perforating pipe of hot fluid (A) and cold fluid (B).

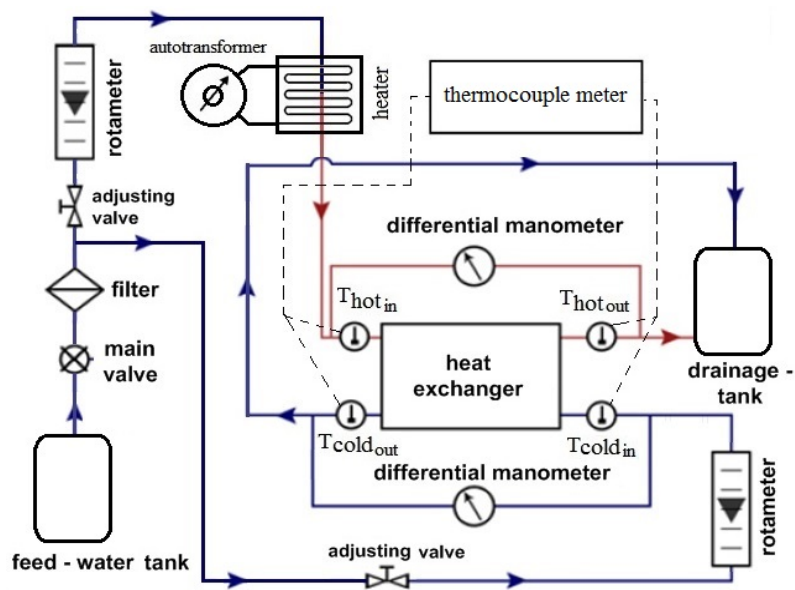


**Figure 3** Schematic view of the test stand in water-water configuration.

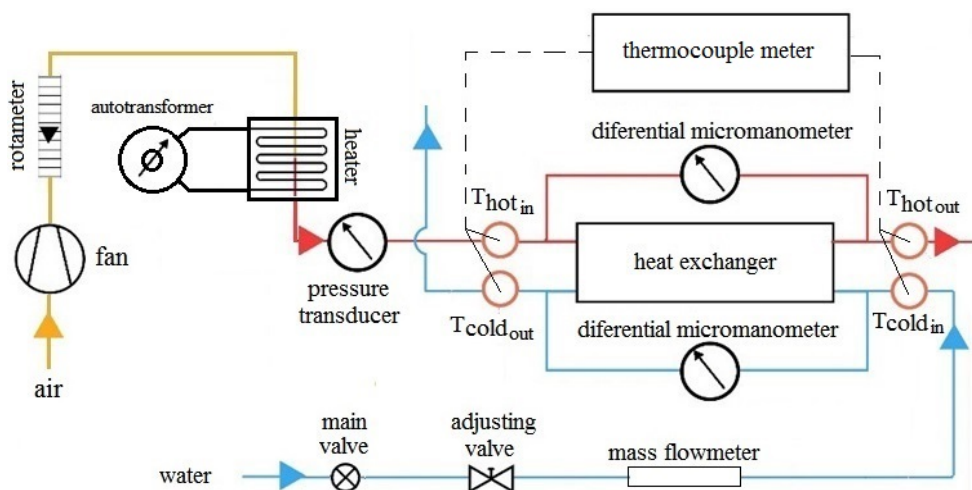


**Figure 4** Schematic view of the test stand in gas-water configuration.

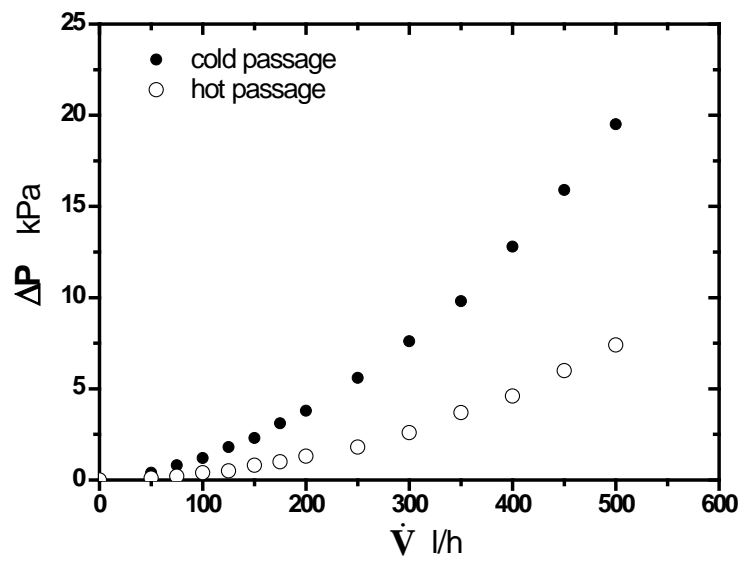


**Figure 5** Flow characteristics of MJHE in water–water configuration.



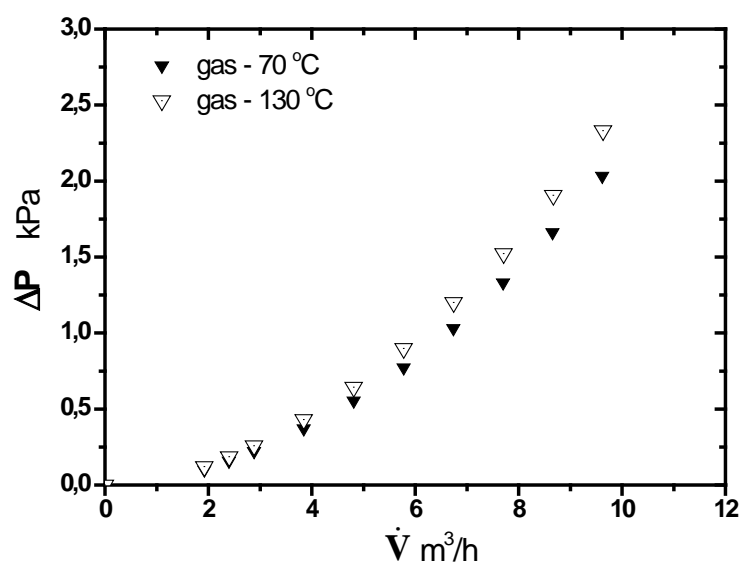


**Figure 6** Gas side flow characteristics in gas-water configuration.

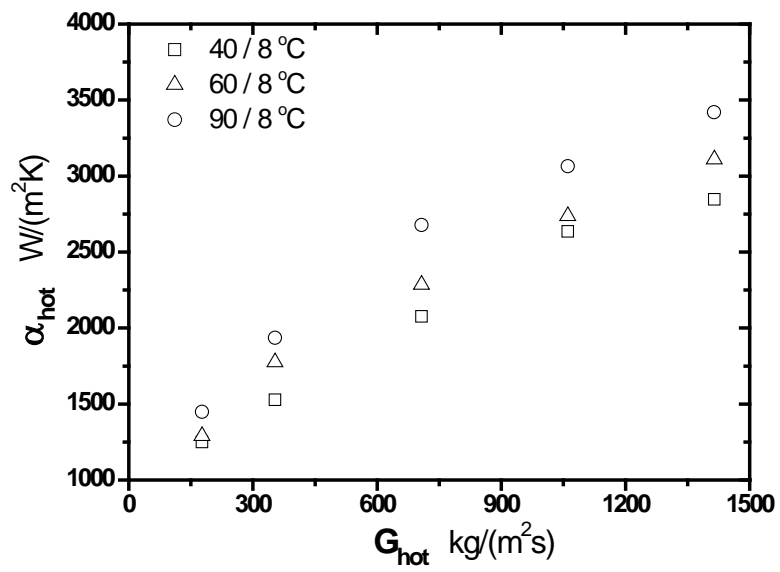


**Figure 7** Heat transfer coefficients versus the mass flux for hot passage at the case of water–water configuration.

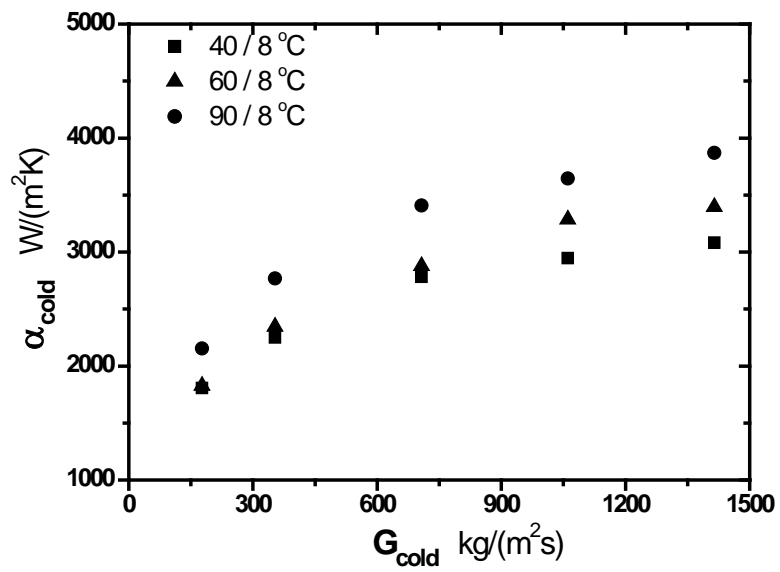


**Figure 8** Heat transfer coefficients versus the mass flux for cold passage at the case of water–water configuration.

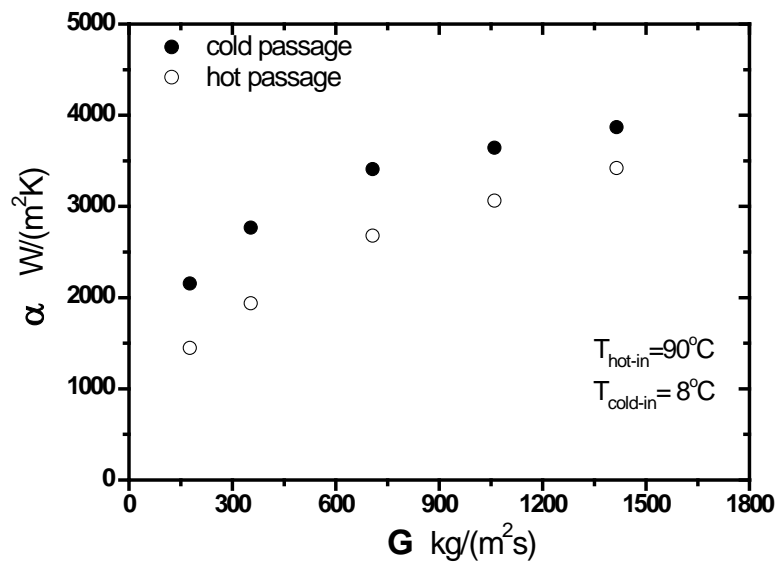


**Figure 9** Comparison of heat transfer coefficients as the mass flux function for the case of water–water configuration at selected temperature difference.

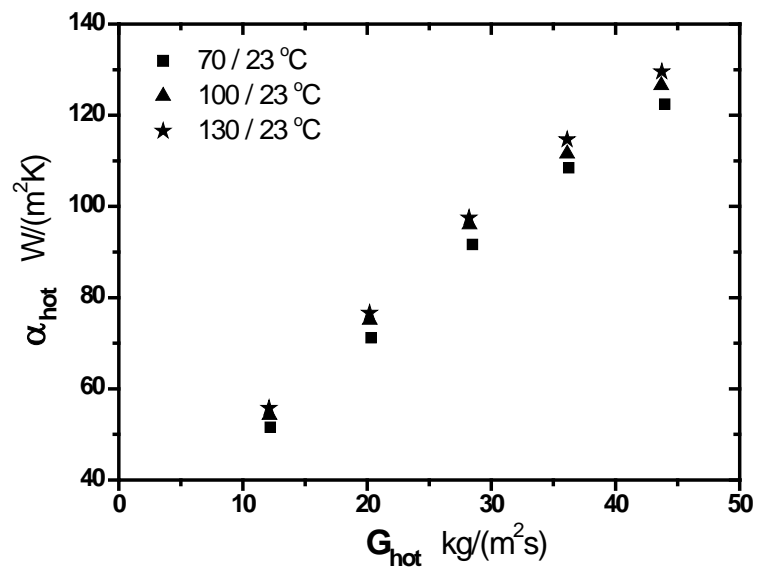


**Figure 10** Heat transfer coefficients versus the mass flux for hot passage at the case of gas–water configuration.

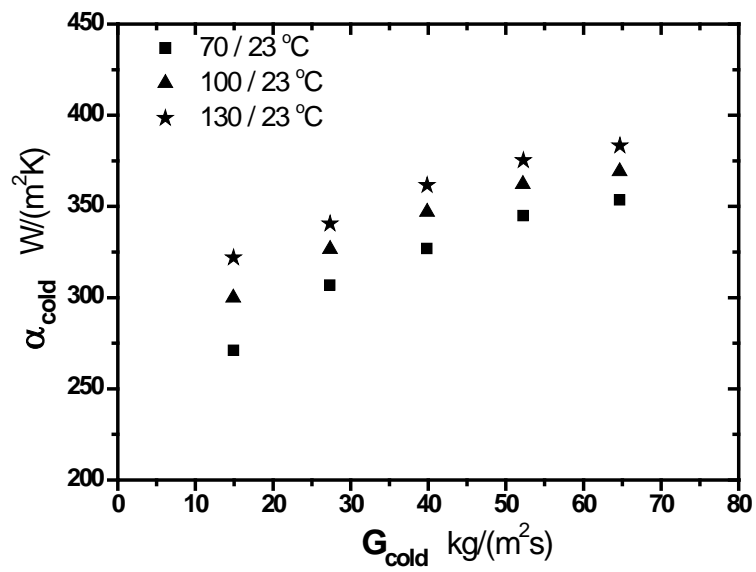


**Figure 11** Heat transfer coefficients versus the mass flux for cold passage at the case of gas–water configuration.

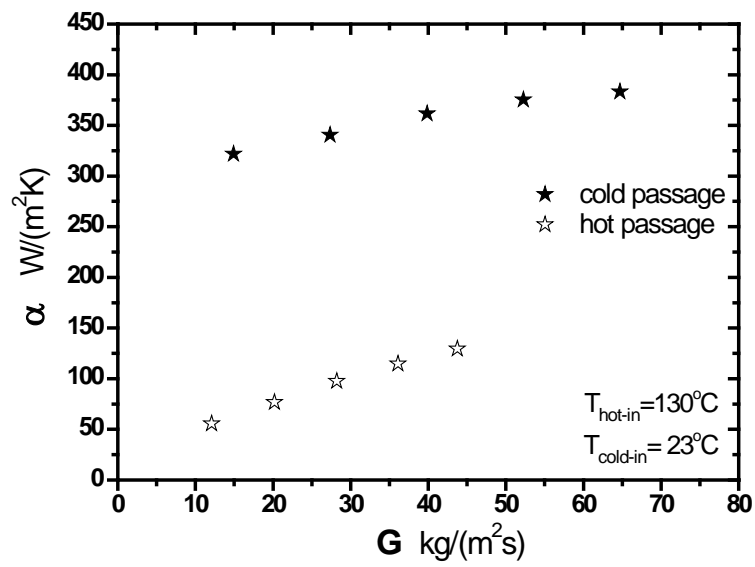


**Figure 12** Comparison of heat transfer coefficients as the mass flux function for the case of gas–water configuration at selected temperature difference.

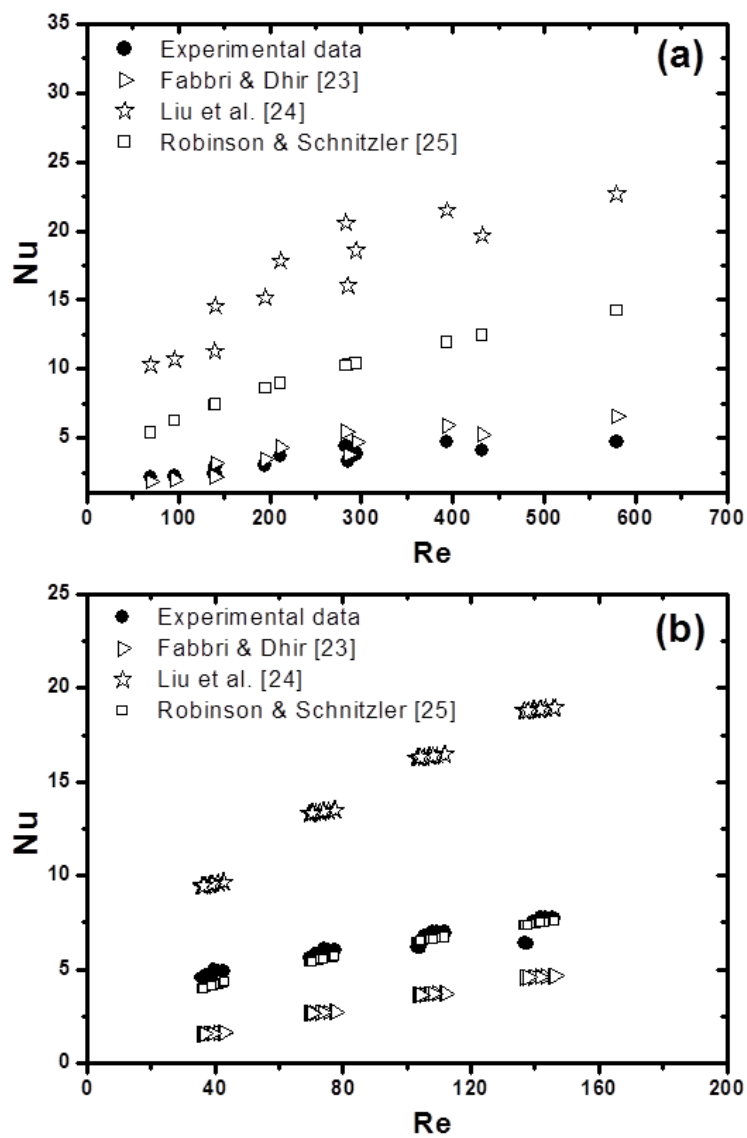


**Figure 13** Nusselt number versus Reynolds number for water –water configuration, hot (a) and cold (b) passages.



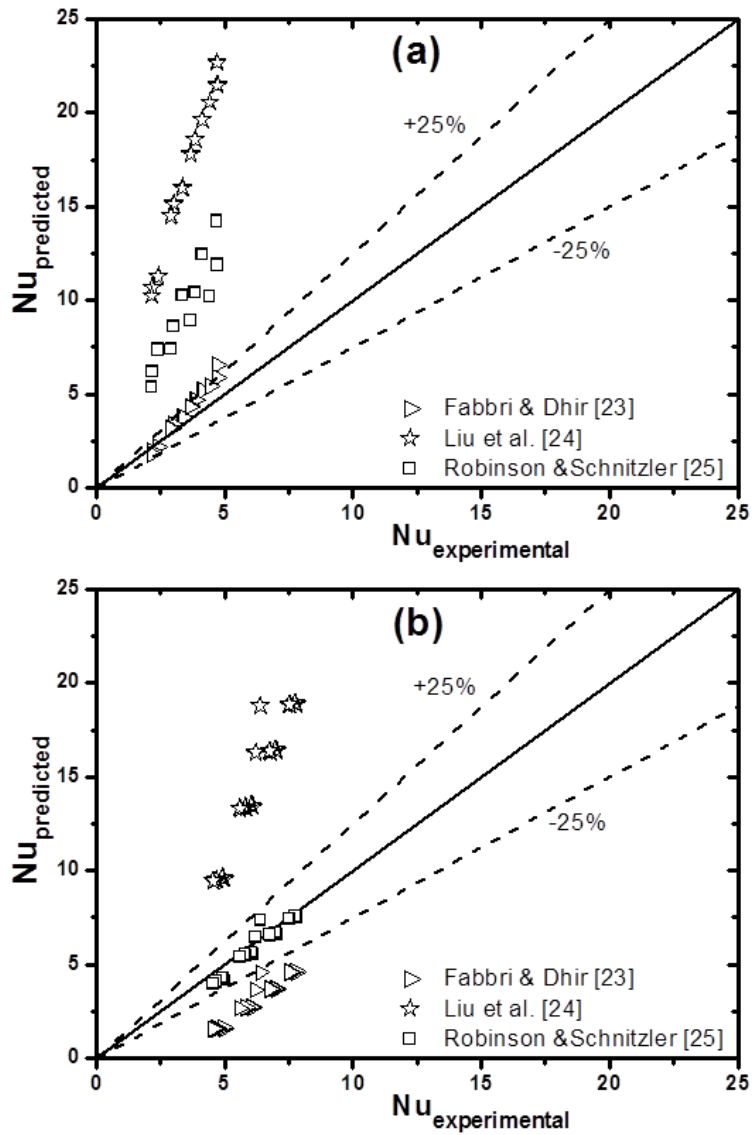


**Figure 14** Comparison of Nusselt number predictions with the presented in this paper experimental data for water –water configuration, hot (a) and cold (b) passages.

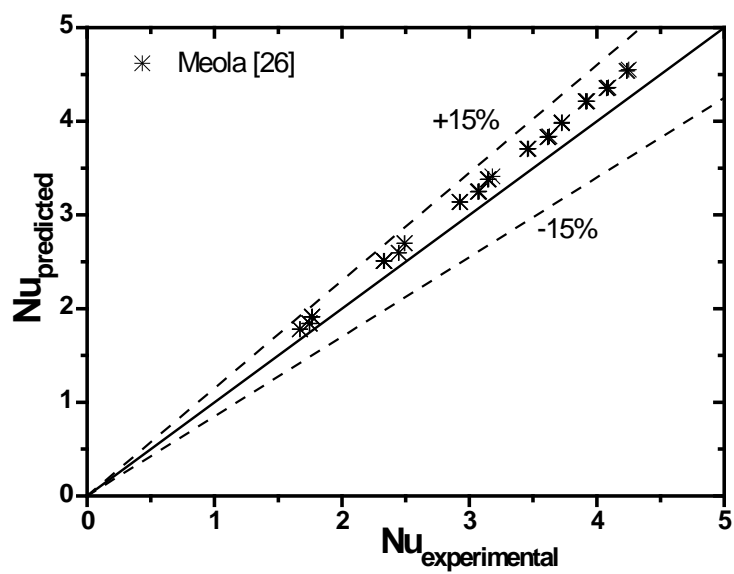


**Figure 15** Comparison of the Nusselt number prediction by Meola [26] with the experimental data for gas –water configuration, hot passage.



**Jan Wajs** is a research fellow at the Faculty of Mechanical Engineering of Gdansk University of Technology, Poland. He received his M.Sc. and Ph.D. degrees from Gdansk University of Technology in 2000 and 2007, respectively. Since 2000 he has been teaching at the GUT. In 2011-2014 he also worked as an expert at the Institute of Fluid-Flow Machinery PAS. The areas of his research activity include experimental investigations and mathematical modeling of heat transfer during flow boiling and condensation at a large scale and in minichannels, designing of compact heat exchangers (based on minichannels, microjets) and heat recovery systems based on the organic Rankine cycle for industrial and domestic applications.



**Dariusz Mikielwicz** is a professor of thermal sciences at the Faculty of Mechanical Engineering of Gdansk University of Technology, Gdansk, Poland. He received his MSc. degree from the Gdansk University of Technology (1990), and PhD. degree from the University of Manchester (1994). In 2002 he presented his habilitational dissertation at the Gdansk University of Technology. In 1994–1996 he worked as an engineer at the Berkeley Nuclear Laboratories, Gloucestershire, UK. Since that time he has been teaching at the GUT. He had placements at the Institute of Fluid-Flow Machinery PAS. His research interest is in the field of modeling of two-phase flows during both boiling and condensation, efficient and precise jet and microjet cooling of hot surfaces, and recently heat recovery from low-temperature sources and high temperature heat pumps.



**Elzbieta Fornalik-Wajs** is a research fellow at the Faculty of Energy and Fuels of AGH University of Science and Technology in Krakow, Poland. She received her MSc degree (1996) and PhD degree (2000) from AGH University of Science and Technology. In 2010 she presented her habilitation dissertation at Silesian University of Technology. Since 2000 she has been teaching at the AGH. She is the EIT InnoEnergy PhD School Officer for Poland from 2014. Her research interests are directed but not limited to: experimental and numerical investigations of heat and mass transfer, fluid mechanics related phenomena (impinging jets, heat transfer processes in turbulent confined jets, convection in Czochralski melt systems, magnetic convection, nanofluids, heat exchangers), thermodynamics and energy systems.



**Michał Bajor** is a PhD student at the Faculty of Mechanical Engineering of Gdansk University of Technology. He received his M.Sc. degree from GUT in 2013. The areas of his research activity include experimental investigations and mathematical modeling of single-phase jet impingement heat transfer in compact heat exchangers.